Journal of Materials and Environmental Science
ISSN : 2028-2508
e-ISSN : 2737-890X
CODEN : JMESCN

J. Mater. Environ. Sci., 2023, Volume 14, Issue 7, Page 811-825

http://www.jmaterenvironsci.com

Investigation of Corrosion Inhibition behaviour of 3-Methyl-5-Phenylisoxazole on Mild Steel Surface in HCl Solution

Kufre E. Essien[1,*], Ekerete J. BoEkom[2], Okon E. Okon[3], Anduang O. Odiongenyi[1], Idongesit George[3], Effiong J. Okon[3]

[1]*Department of Chemistry, Faculty of Physical Sciences, Akwa Ibom State University, Mkpat Enin, P.M.B. 1167, Nigeria*
[2] *Department of Chemistry, Faculty of Sciences, University of Uyo, Uyo, P.M.B. 1017, Nigeria*
[3]*Department of Chemical Sciences, Akwa Ibom State Polytechnic, Ikot Osurua, P.M.B. 1200, Nigeria*

* *Corresponding author, Email address: kufreessien@aksu.edu.ng*

Received *03 June 2023,*
Revised *11 July 2023,*
Accepted *13 July 2023*

Citation*: Essien, K. E., BoEkom, E. J., Okon, E. O., Odiongenyi, A. O., Idongesit George, Okon, E. J. (2023) Investigation of Corrosion Inhibition behaviour of 3-Methyl-5-Phenylisoxazole on Mild Steel Surface in HCl Solution, J. Mater. Environ. Sci., 14(7), 811-825.*

Abstract

The exploration for green corrosion inhibitor for mild steel in a 2 M HCl solution was carried out by using gravimetric, quantum, and IR surface analyses at 303 K – 333 K. The anti-corrosion ability of 3-Methyl-5-Phenylisoxazole (MPI) was established and the results obtained disclosed that inhibition efficiency increased with an increase in inhibitor concentrations. The maximum inhibition at the optimum concentration in HCl solution at 303 K was 72 %. The adsorption of MPI molecule on mild steel obeys the Temkin adsorption isotherm at all studied temperatures with negative values of ΔG^{o}_{ads}, suggesting a stable and spontaneous inhibition process. Quantum chemical calculations revealed that this compound, apart from meeting the basic requirements for corrosion inhibition, they are also characterized by frontier molecular energy values that are unique for well-known corrosion inhibitors. The Fukui index was proposed to foresee electrophilic and nucleophilic sites of the inhibitor molecule. The Fourier-transformed infra-red spectrophotometer was used to identify the functional groups participating in the inhibition process. The adsorption of MPI molecules on the mild steel surfaces was confirmed using FTIR results.

Keywords: *3-Methyl-5-Phenylisoxazole; Mild steel; Temkin isotherm; Corrosion; Adsorption*

1. Introduction

Industries counter a lot of challenges due to the corrosion of iron-based materials. Hence, the protection of Iron-based materials against corrosion calls for urgent attention**.** This trend to protect Iron-based materials against corrosion has been advanced with numerous methods. One of the most realistic methods to protect Iron-based materials against corrosion is the use of inhibitors. However, it has been ascertained by a lot of researchers that organic compounds are effective corrosion inhibitors for metals due to the existence of a high electronic density such as oxygen, sulphur, and nitrogen atoms, as well as π electrons in triple or conjugated double bonds (Udhayakala *et al*., 2012; Fouda and Ellithy, 2009; Tebbji *et al*., 2007; Bouklah *et al*., 2006).

Among numerous organic inhibitors, azole compounds have gotten great consideration. Indeed, several azole derivatives have been reported to be effective corrosion inhibitors for steel and copper in acidic media (Antonijević *et al*., 2009; Anusuya *et al.*, 2015; Obot and Obi-Egbedi, 2010). Many azole derivatives such as oxazole (Rahmani *et al*., 2018), pyrazole (El-Hajjaji *et al*., 2018; El Arrouji *et al.,*

2016; Guendouz *et al.*, 2013), and Benzimidazole (Rahmani *et al.*, 2018) compounds have been recently studied as corrosion inhibitors for mild steel in hydrochloric acid, and have been shown good inhibition properties. Azole derivatives are one of the important classes of heterocyclic compounds which have various applications in several fields. The effectiveness of corrosion inhibition of azolic compounds in certain aggressive environments for mild steel has been established by many researchers over the past decades (El Arrouji *et al*., 2020; Glaser *et al.*, 2000; Yadav *et al*., 2016). Mechbal *et al.* (2021) reported the corrosion prohibition capacity of two synthesized eco-friendly pyrazole derivatives namely, N1, N1, N5,N5-tetrakis(3,5-dimethyl-1H-pyrazole-1-yl)methyl)naphthalene-1,5-diamine (NPDM) and N1,N1,N5,N5-tetrakis(1H-pyrazole-1-yl) methyl)naphthalene-1,5-diamine (NPD) has impressive IEs of 89.02 % and 92.10 % at 10^{-3} mol/L in 0.5 M H_2SO_4. Rahmani *et al.* (2018) reported the corrosion inhibition performances of (4-ethyl-2-phenyl-4,5-dihydro-1,3-oxazol-4-yl)- methanol (C1); 4-{[(4-ethyl-2-phenyl-4,5-dihydro-1,3-oxazol-4-yl)methoxy]methyl}- benzene-1-sulfonate (C2) and 4-[(azidoxy)methyl]-4-ethyl-2-phenyl-4,5-dihydro-1,3- oxazole (C3) mild steel in molar hydrochloric solution. Benzai *et al.* (2021) reported the study of the inhibition of mild steel corrosion in a molar hydrochloric acid medium by some benzoxazole derivatives compounds. The excellent reactivity of oxazole compounds to form complexes with metallic ions is also studied Benzai *et al.* (2019). The inhibition performance of 5-methyl-3-phenylisoxazole-4-carboxylic acid (MPC) alone and in combination with potassium iodide (KI) for low carbon steel in 1.0 M HCl and H_2SO_4 solutions have been studied by Solomon et al. (Solomon *et al*., 2022). Results obtained indicate that the optimum concentration of MPC in 1.0 M HCl and H_2SO_4 solutions is 500 mg/L and 50 mg/L, respectively. The maximum inhibition at the optimum concentrations of MPC in HCl and H_2SO_4 solutions at 25°C is 46% and 23%, respectively. The addition of 3 mM KI to 500 mg/L MPC in HCl solution and to 50 mg/L MPC in H_2SO_4 solution at 25°C raised the inhibition efficiency to 86% and 89%, respectively.

In the current paper, we are to explore the corrosion inhibition properties of 3-Methyl-5-phenylisoxazole in 2 M HCl by using gravimetric, computational, and IR methods of analysis. The selection of the 3-Methyl-5-phenylisoxazole for this study was from the accomplishment of the crucial requirements of corrosion inhibitors as reported by Umoren (Umoren, 2008). Also, it has not been used as a mild steel corrosion inhibitor in an acidic medium to the best of our knowledge. The study shall involve investigating the corrosion inhibition properties of the 3-Methyl-5-phenylisoxazole for mild steel in an acidic medium. Moreso, it is anticipated that with the multiple adsorption sites, they shall be able to form complexes with the metal ions and on the metal surface (Umoren, 2011). The adsorption of organic compounds on the metallic substrate developed a thin protective layer, which brings about the protection of the metal from the corrosive attack of the surroundings (Chauhan *et al.*, 2021). A comparative study was carried out to inspect the inhibition doings of this derivative about their molecular geometries (extent of planarity), and global and local electronic properties in a destructive acid-aqueous medium. This study shall aid the understanding of corrosion mechanisms and minimize corrosion problems. The molecular structure of the studied compound is shown in Figure 1 and the compound was purchased from Sigma Aldrich.

2. Methodology

2.1 Gravimetric experiments

The SiC abrasive papers, 320, 400, and 600 grit were used in polishing the mild steel coupons for the gravimetric experiment. The polished coupons were degreased in absolute ethanol, dried in acetone, and stored in moisture-free desiccators before use (Oguzie *et al.*, 2012). Corresponding concentrated solutions were used to prepare different concentrations (2.0×10^{-4} M – 10×10^{-4} M) of 3-Methyl-5-

phenylisoxazole and the solutions in the absence of 3-Methyl-5-phenylisoxazole were taken to be blank. The pre-cleaned and weighed coupons were immersed in beakers containing 100 ml test solutions maintained at 303 – 333 K.

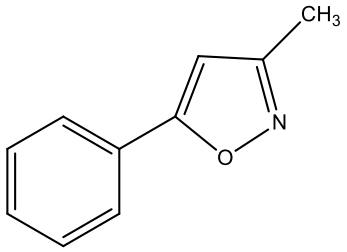

Figure 1: Chemical Structures of 3-Methyl-5-phenyl isoxazole

Weight loss was determined by removing the coupons from test solutions at 2 h intervals progressively for 10 h, washing them in distilled water, scrubbing them with a bristle brush, drying them in acetone, and re-weighed (Oguzie *et al*., 2012). The weight loss was taken to be the difference between the initial weight and the weight of the coupons at a given time interval.

2.2 Molecular modeling

Quantum chemical calculations were used to study corrosion inhibition mechanisms. Thus, the verification was done to know the possible physical properties which could contribute to inhibition. Full optimization was done using molecular mechanics, *Ab initio,* and DFT level (Eddy *et al*., 2015). PM7 Hamiltonian in the MOPAC 2014 software was used in computing semi-empirical parameters for the molecules (Ebenso *et al.,* 2010). Single-point DFT calculations were also carried out using Hyperchem release 8.2 packages. DFT setting (MP2 inclusive) in the package were Basic set: 321-G, iteration = 50, spin pairing = unrestricted Hartree Fock, convergence limit = 1E-0.05, and Spin multiplicity = 1 (for zero charges and 2 for +1 and -1 charges). There was concern between the inhibition efficiency of this inhibitor and the quantum chemical parameters (Eddy *et al.*, 2010).

2.3 Surface Characterization

The results of corrosion tests were best understood using the coatings. Microstructural features were identified by using Fourier Transform Infra Ray (FT-IR). The surfaces of the corroded samples were observed after 24 h of immersion in the respective corrosive medium. The IR spectra were recorded for the MPI solution and 2M HCl solution after 24h of mild steel sample immersion at 30° C.

3. Results and Discussion

3.1 Weight loss studies

The propensity of the 3-Methyl-5-phenylisoxazole (MPI) to minimize mild steel corrosion in the acidic medium was ascertained using the gravimetric experiment (Ebenso *et al.*, 2010). From the outcomes in Table 1, weight loss measurement increases with an increase in time but decreased with an increase in concentrations of the 3-Methyl-5-phenylisoxazole. A lot of researchers observed a similar trend (Cherrak *et al*., 2021; Echihi *et al*., 2021; El Arrouji *et al.*, 2020; Hosseini *et al.*, 2010; Njoku *et al.*, 2019; Tebbji *et al.*, 2005). Figure 2 demonstrated the weight loss measurements with time at 303 K and related trends were observed at 313, 323, and 333 K.

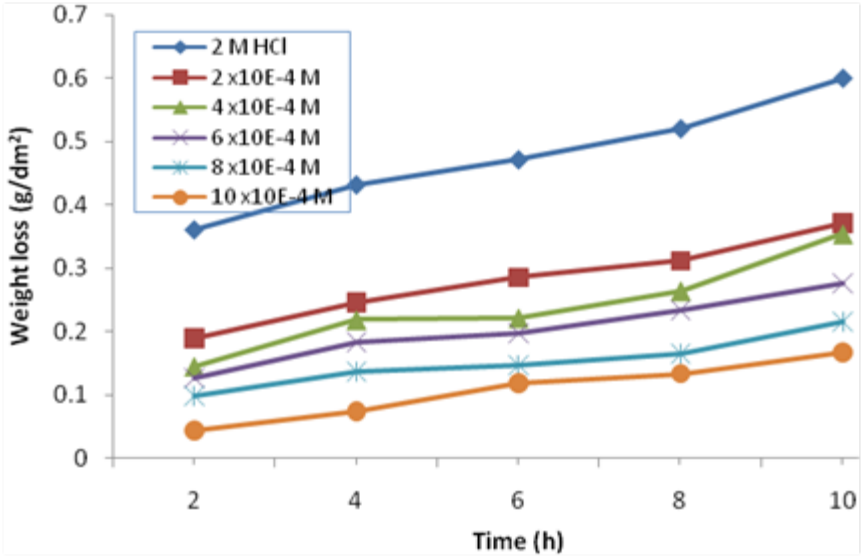

Figure 2: Plot of weight loss versus time (hr) in the absence and presence of different concentrations of MPI at 303 K.

A maximum inhibition efficiency of 72 % at the optimum concentration of 10 x 10^{-4} M at 303 K was exhibited by the studied compound (Table 1). Hence, the studied inhibitor was found to be more effective at 303 K (Table 1) (Hosseini *et al*., 2010). This result corresponds to that of Paul *et al*. (2020), Essien and Abai (2022), and Dohare *et al*. (2019), and is attributed to partial desorption of the molecules from the mild Steel surface.

Table 1: Calculated values of corrosion rate (CR), surface coverage (θ), and inhibition efficiency (%I) of mild steel corrosion in different concentrations of MPI

	303 K			**313 K**			**323 K**			**333 K**		
Conc. of [MPI] (M) x 10^{-4}	CR (mm/yr) x 10^{-3}	θ	I (%)	CR (mm/yr) x 10^{-3}	θ	I (%)	CR (mm/yr) x 10^{-3}	θ	I (%)	CR (mm/yr) x 10^{-3}	θ	I (%)
Blank	3.00	-	-	4.96	-	-	6.34	-	-	8.41	-	-
2	1.86	0.38	38	3.77	0.24	24	5.14	0.19	19	7.06	0.16	16
4	1.77	0.41	41	3.32	0.33	33	4.63	0.27	27	6.31	0.25	25
6	1.38	0.54	54	2.73	0.45	45	3.80	0.40	40	5.38	0.36	36
8	1.08	0.64	64	2.23	0.55	55	3.04	0.52	52	4.54	0.46	46
10	0.84	0.72	72	1.79	0.64	64	2.35	0.63	63	3.70	0.56	56

3.2 Effect of temperature

The temperature dependence of corrosion rates in uninhibited and inhibited solutions was studied in the presence of different concentrations of MPI in 2 M HCl solutions (Dohare *et al*., 2019). The results show that inhibition efficiency increased with the concentration of inhibitor (Njoku *et al*., 2016). Similar behavior was reported by several researchers (Dohare *et al*., 2019; El Ouadi *et al*., 2021; Essien and Abai, 2022; Ouchrif *et al*., 2005; Paul *et al*., 2020; Verma *et al*., 2020). High efficiency of 72 % was noticed after 10 h, which points out, that the surface coverage of the substrate by these inhibitors attended an optimum level within 10 h. The results show that inhibition efficiency decreases as the temperature increases indicating the physisorption process as reported by Khaled *et al*., 2012. The mechanism of adsorption was studied using adsorption isotherms (Jackson *et al*., 2016; Jackson and

Essien, 2019; Obot *et al*., 2010). Adsorption isotherms gave vital information on the interaction of inhibitor and metal surfaces as observed by Umoren (2008) and Essien and Abai (2022). The degree of surface coverage values (θ) at different inhibitor concentrations in 2 M HCl solutions were assessed from weight loss measurements at 303 – 333 K and tested graphically for fitting to a suitable adsorption isotherm (Obi-Egbedi *et al.*, 2011a, 2011b; Tang *et al*., 2006). The adsorption isotherm model considered was Temkin isotherm as represented by equation (1) (Obi-Egbedi *et al.*, 2011b):

$$\exp(f\theta) = K_{ads}C \qquad (1)$$

Where K_{ads} is equilibrium, constant of the adsorption process, C is inhibitor concentration and f is a factor of energetic inhomogeneity. The equilibrium, K_{ads} was calculated from the slope of θ versus ln C graph as shown in Figure 3. Among the adsorption isotherm models considered, the best-fitted straight line was obtained from the Temkin isotherm as the correlation coefficients (R2) were in the range of $0.9993 \geq R2 \geq 0.9756$. From the results in Table 2, it is seen that the values of molecular interaction parameter 'a' are negative in all cases showing attraction in the adsorption layer. A similar result was observed by Obot and Obi-Egbedi (2008). The equilibrium constant of the adsorption process, K_{ads} denotes the strength between adsorbate and adsorbent. The higher the values of K_{ads}, the more efficient the adsorption and hence, better inhibition efficiency (Abd El Rehim *et al*., 2001). It is obvious from Table 2 that values of K_{ads} are very low indicating weak interaction between the inhibitor and the mild steel surface. This implies that electrostatic interaction (Physisorption) has taken place between the inhibitor molecules and the metal surface (Eddy, 2010; Obi-Egbedi *et al.*, 2011b). The negative values of $\Delta G°_{ads}$ observed in Table 2 reveal that the adsorption of the inhibitors on a mild steel surface in 2 M HCl solution is a spontaneous process (Fouda *et al*., 2006).

Table 2: Adsorption parameters from Temkin isotherm for Mild steel coupons in 2 M HCl containing different concentrations of MPI at 303 - 333 K.

Temp. (°C)	**Adsorption parameters**						
	Intercept	Slope	K (mol/l)	f	a	-ΔG (KJ/mol)	R^2
30	0.265	0.091	18.36	10.99	-5.50	17.45	0.9756
40	0.136	0.102	3.78	9.80	-4.90	13.91	0.9977
50	0.063	0.113	1.75	8.85	-4.43	12.29	0.9954
60	0.055	0.101	1.72	9.90	-4.95	12.62	0.9993

The presence of MPI increases the activation energy of the metal dissolution reaction as shown in table 3. The presence of the inhibitor results in the blocking of the active sites which leads to an increase in the activation energy of mild steel corrosion in the inhibited state (Soltani *et al.*, 2014). The higher value of E_a in the presence of inhibitors compared to that in its absence and the decrease in the inhibition efficiency (%) with rising in temperature is deduced as an indication of physisorption (Obi-Egbedi *et al*., 2011a). The corrosion rate relates to temperature in an acidic solution by the Arrhenius equation as shown in equation (2).

$$\text{Log CR} = \text{Log A} - E_a/2.303RT \qquad - \qquad - \qquad 2$$

where CR is the corrosion rate, E_a, is the apparent activation energy, A the Arrhenius constant, R is the molar gas constant and T is the absolute temperature (Essien and Abai, 2022). The apparent activation energy was determined from the slopes of log CR versus I/T graphs depicted in Figure 4.

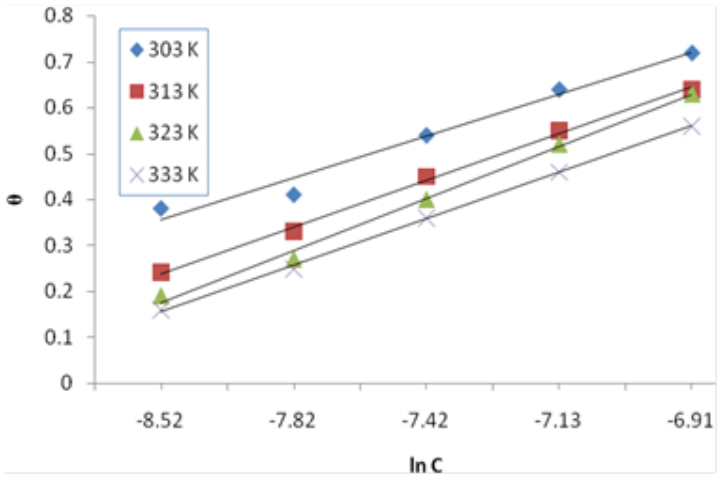

Figure 3: Temkin adsorption isotherm plot θ versus ln C for Mild steel coupons in 2 M HCl solution containing different concentrations of MPI.

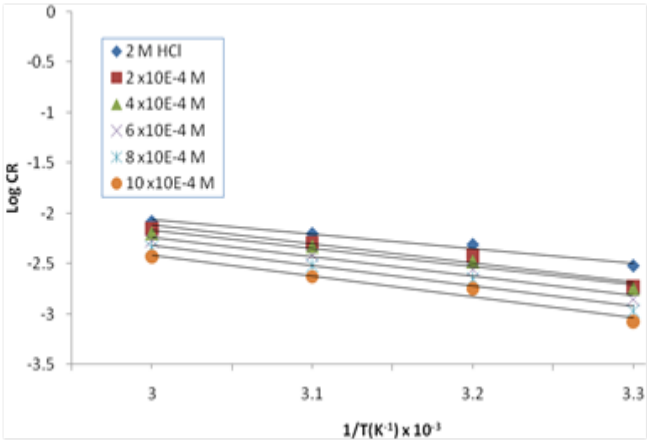

Figure 4: Arrhenius plot as log CR versus 1/T for mild steel coupons in 2 M HCl containing different concentrations of MPI.

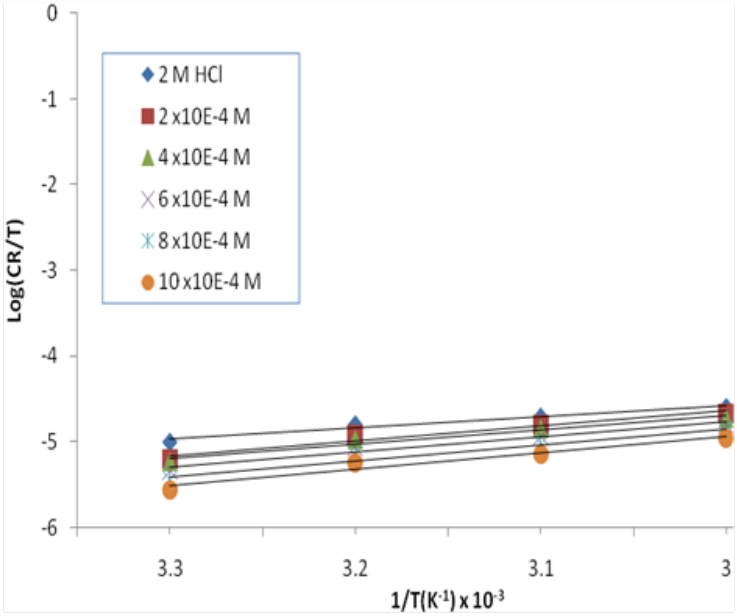

Figure 5: Transition State plot as the log (CR/T) versus 1/T for mild steel coupons in 2 M HCl containing different concentrations of MPI.

The activation parameters were determined from the slope of the log (CR/T) versus the 1/T graph depicted in Figure 5. The computed values of the activation parameters for the dissolution of mild steel at different temperatures are presented in Table 3. Table 3 revealed that the positive values of ΔH^o reflect the endothermic behavior of the adsorption of the studied inhibitor on the mild steel surface (Tang *et al.*, 2006). The ΔS^o values are negative indicating that the adsorption is an endothermic process (Umoren, 2008). The adsorption between the organic compound in the aqueous phase [org (sol)] and water molecules at the electrode surface [H_2O(ads)] is regarded as a quasi-substitution process (Fouda *et al.*, 2006). Thus, the adsorption of MPI molecules is accompanied by the desorption of water molecules from the electrode surface.

Table 3: Activation parameters for Mild steel in 2 M HCl containing different concentrations of MPI at 30-60°C.

MPI Conc (M) x 10^{-4}	ACTIVATION PARAMETERS			
	ΔH (kJ/mol)	- ΔS (J/mol K^{-1})	E_a (kJ/mol)	A x 10^{-3} (J/mol K^{-1})
Blank	1.089	1062	3.776	12.220
2	1.422	1060	3.842	11.940
4	1.472	1060	3.857	11.561
6	1.555	1059	3.849	11.324
8	1.630	1059	4.021	11.220
10	1.671	1058	4.117	10.328

The thermodynamic parameters obtained are the algebraic sum of the adsorption of these organic molecules and the desorption of water molecules (Soltani *et al.*, 2014). Thus, the increase in entropy is due to the increase in solvent entropy (Emranuzzaman *et al.*, 2004). The negative values for entropy imply that the adsorption process is attended by a decrease in entropy, which is the driving force for the adsorption of MPI on the mild steel surface (Li *et al.*, 2014). The difference between E_a and ΔH is about 2.4 kJ/mol indicating that the reduction of H^+ leads to H monatomic to form after H_2 (Batah *et al.*, 2017; Rguiti , 2018)

3.3 Global molecular reactivity

The quantum chemical parameters computed with PM7 Hamiltonian in the MOPAC 2014 software using the gas phase for the studied compounds are presented in Table 4. Similar software has been used by Eddy (2011) and Ikot *et al.* (2009). The difference between the energy of the highest occupied molecular orbital (E_{HOMO}) and that of the lowest unoccupied molecular orbital (E_{LUMO}) are important parameters for defining the reactivity of a chemical species (Ikot *et al.*, 2009). A smaller energy gap implies high reactivity to a chemical species (Eddy, 2011; Essien and Abai, 2022; Obi-Egbedi *et al.*, 2011b; Obot *et al.*, 2021). From Table 4, it is obvious that the energy gap, ΔE of the studied inhibitor is 8.624 eV. As a result, the inhibition efficiency of the inhibitor molecule is 72 %. Figures 6 and 7 showed the distribution of HOMO and LUMO of the 3-Methyl-5-phenylisoxazole molecule. From Figures 6 and 7, it could be seen that the distribution of HOMO and LUMO is mainly located at the oxazole ring, nitrogen, and oxygen atoms in substituent groups. This kind of distribution favors the parallel adsorption of oxazole derivative inhibitor onto the metal surface via two modes (Yadav *et al.*, 2014). One mode is that the inhibitor molecules donate electrons to the unoccupied d orbital of the Fe atom forming a coordinate bond and the other mode is that the inhibitor molecules accept electrons from the Fe atom to form a back-donating bond (Deng *et al.*, 2014). Besides, the expected trend for the variation of inhibition efficiency is consistent with the experimental results.

Table 4: PM7 semi empirical parameters for the 3-Methyl-5-phenylisoxazole molecule

Semiempirical Parameters (eV)	MPI
H_f (kCal/mol)	35.82
TE (eV)	-1829.40
EE (eV)	-9558.84
CCR (eV)	7729.45
Dipole (eV)	2.96
IE (eV)	9.42
E_{HOMO} (eV)	-9.412
E_{LUMO} (eV)	-0.788
E_{L-H} (eV)	8.624
Cosmo area ($Å^2$)	195.93
Cosmo volume ($Å^3$)	194.55
Hydration energy (kCal/mol)	-3.35
Log P	1.52
Refractivity ($Å^3$)	52.68
Polarizability ($Å^3$)	18.38

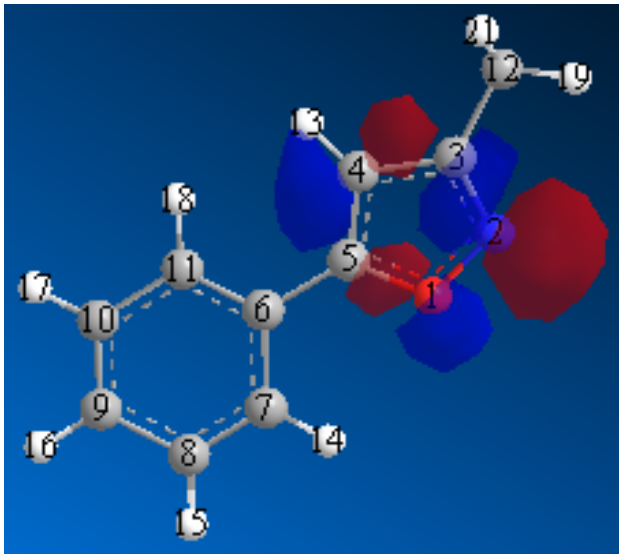

Figure 6: HOMO electronic density of 3-Methyl-5-phenyl isoxazole molecule

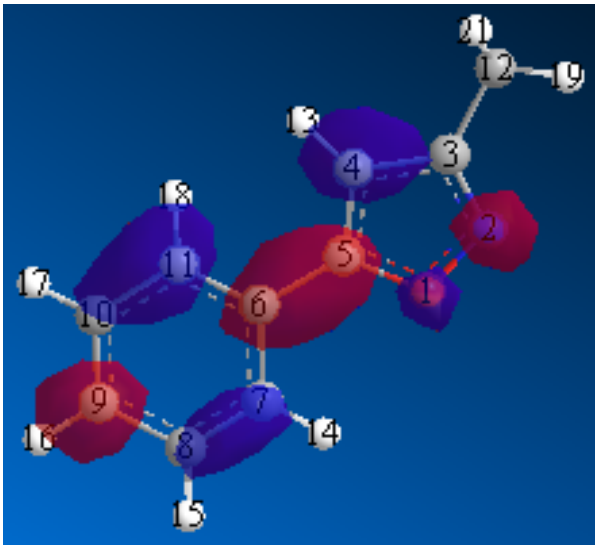

Figure 7: LUMO electronic density of 3-Methyl-5-phenyl isoxazole molecule

Semiempirical calculations estimate ionization energy through the value of E_{HOMO}. Ionization energy measures the ability of a molecule to lose electrons. In this case, two systems, Fe (in mild steel) and inhibitor are brought together, hence, electrons will flow from the lower system with lower electronegativity (inhibitor) to the system with higher electronegativity until the chemical potential becomes equal (Eddy, 2011). Based on the IE, the trend for the variation of inhibition potentials of the studied oxazole derivative agrees with experimental findings.

Log P is a substituent constant accounting for the hydrophobicity of the actual molecule. The hydrophobicity of organic molecules increases with decreasing water solubility. In corrosion studies, hydrophobicity is related to the mechanism of formation of the oxide/ hydroxide layer on the metal surface (which reduces the corrosion process drastically) (Ebenso *et al.*, 2010; Eddy, 2011).

The dipole moment of a compound (μ) refers to the tendency of a system to act as a dipole. The dipole moment is the measured polarity of a polar covalent bond (Eddy, 2010). It is defined as the product of the magnitude of the charge on the atoms and the distance between the two bonded atoms. From Table 4, the negative total energy indicates that the studied inhibitor is a very stable molecule and is less prone to be broken apart. The dipole moment of the studied inhibitor is 2.96 Debye which is higher than that of H_2O (1.87 Debye) (Eddy, 2010). The high values of dipole moment probably increase the adsorption between the compound and the metal surface. Moreover, effective adsorption of the studied molecules on the mild steel surface is enhanced by higher area and volume. Literature discloses that there are several abnormalities in the correlation involving dipole moment and inhibition efficiency, noting that core-core repulsion (C–C) energy is a quantum chemical parameter that has a tremendous correlation with inhibition efficiency (Eddy, 2010; Essien and Abai, 2022). The HOMO and LUMO molecular orbitals of the studied molecules are shown in Figures 6 and 7 respectively. The blue and maroon orbital represent positive and negative sites of adsorption respectively.

3.4 Local molecular selectivity

The local molecular selectivity of the 3-Methyl-5-phenylisoxazole molecule was analyzed by condensed Fukui and condensed softness functions. The indices that allowed the distinction of each part of a molecule based on its chemical behavior due to different substituent functional groups were condensed Fukui and the condensed softness functions (Dohare *et al.*, 2019; Eddy, 2011). Local molecular reactivity was used to evaluate the active sites of the inhibitor molecules. Table 5 showed the local reactivity parameters of the studied inhibitor.

Table 5: Fukui functions for carbon and electronegative elements in 3-Methyl-5-phenyl isoxazole

Atom No.	q_{Huckel}	q_N	q_{N-1}	q_{N+1}	f_k^-	f_k^+	$f^{(2)}(\mathbf{r})$
O(1)	0.058591	0.0271	-0.0294	-0.0118	0.0565	-0.0389	-0.0954
N(2)	-0.215003	0.0484	-0.1723	-0.0148	0.2207	-0.0632	-0.2839
C(3)	0.136265	-0.0354	-0.0080	-0.0508	-0.0274	-0.0154	0.012
C(4)	-0.202224	0.0615	0.0900	0.0460	-0.0284	-0.0155	0.0129
C(5)	0.196663	-0.0004	0.0911	-0.0571	-0.0915	-0.0567	0.0348
C(6)	0.0278805	-0.0410	0.0927	-0.0511	-0.1337	-0.0101	0.1236
C(7)	-0.0317479	0.0461	0.1112	0.0244	-0.0651	-0.0217	0.0434
C(8)	-0.0241282	0.0464	0.0753	0.0315	-0.0288	-0.0150	0.0138
C(9)	-0.0314597	0.0508	0.2114	0.0293	-0.1607	-0.0215	0.1392
C(10)	-0.0244188	0.0408	0.0762	0.0266	-0.0354	-0.0142	0.0212
C(11)	-0.0414661	0.0598	0.1396	0.0374	-0.0798	-0.0224	0.0574
C(12)	-0.0901975	-0.1126	-0.1055	-0.1188	-0.0071	-0.0062	0.0009

The Fukui function is roused from the fact that an electron is transferred to an N electron molecule, and tends to distribute to minimize the energy of the resulting N + d electron system (Eddy, 2011; Ji *et al*., 2016). The resulting change in electron density is nucleophilic and electrophilic. Table 5 presents calculated values of f^+ and f^- for carbon, nitrogen, and oxygen atoms in the MPI molecule. The site for the nucleophilic attack is at the place where the value of f^+ is maximum whereas the site for the electrophilic attack is controlled by the value of f^-. An atom with high f^+ and f^- would have strong interaction with the metal surface by exchanging electrons (Boulhaoua *et al*., 2021). From the f^+ and f^- presented in Table 5, the active sites could be found. As for electrophilic attack index f^+, the active sites of inhibitor MPI are mainly located on C(7), C(9), C(11), and O(1). As for nucleophilic attack f^- of the studied inhibitor, the active sites are located mostly on the heteroatoms in the substituent groups (Boulhaoua *et al.,* 2021; Dohare *et al*., 2019; Eddy, 2011; Essien and Abai, 2022). The Fukui function is an effective parameter to describe the local reactivity (Deng *et al*., 2014). From the results in Table 5, it could be seen that some atoms possessed both high f^+ and high f^-, which meant that these atoms had strong a capability to attract and donate electrons (Dohare *et al*., 2019). Therefore, it was difficult to estimate their contribution to exchanging electrons with the metal surface. Herein, another parameter known as a dual descriptor was introduced to resolve this situation. This index was expressed as 'be at the same time an indicator for both the nucleophilic and electrophilic regions of a molecule'. The values of f^2 (r) for the studied molecule are presented in Table 5. This indicated that C(6) and C(9) are the electrophilic sites with f^2 (r) of 0.1236 and 0.1392 respectively. These two atoms accepted electrons from the metal surface, whereas O(1) and N(2) are the nucleophilic sites with f^2 (r) of -0.0954 and -0.2839 respectively.

3.5 Surface Characterization

It is established that IR spectroscopy can be utilized to understand the process of rusting of steel. FT-IR spectrum of surface film on mild steel immersed in the presence and absence of MPI is shown in Figure 8. The results revealed that the mild steel corrosion products in the presence of MPI are IR-active.

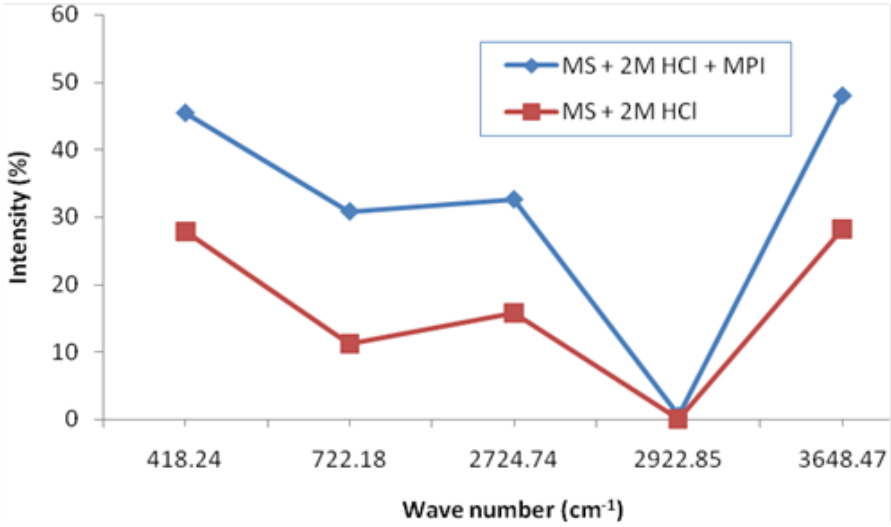

Figure 8: IR spectra for mild steel after corrosion in HCl solution without and with 10 x 10^{-4} M MPI

It has been pointed out that the adsorption band at the higher wavenumber region is due to OH stretching and at the lower wavenumber region is because of Fe-O lattice vibration (Misawa *et al*., 1974, 1971).

From the results, it can be seen that the C-Cl band at 722.11 cm^{-1} in the 2 M HCl spectrum was shifted to 722.18 cm^{-1} in MPI. The C-H stretching band at 2922.75 cm^{-1} in 2M HCl was shifted to 2922.85 cm^{-1} MPI spectra. By comparing the spectra of the HCl solution with that of the MPI inhibitor, we can conclude that some peaks have shifted to higher frequency regions. The presence of these bands in the surface film indicates the existence of MPI molecules in the surface film. The shifts in the stretching frequencies of various functional groups present in the inhibitor molecule are resulted due to the involvement of the molecule in the complex formation. Similarly, the bands at 3419.51 cm^{-1} in 2 M HCl and 3648.47 cm^{-1} in MPI IR spectra are contributed by the –OH group present in possibly traces of ferric hydroxide present in the inhibited film. Ishii *et al.* (1972) also confirmed that the Fe-O stretching vibration in $Fe_{3-x}O_4$ corresponds to wave number, 400-600cm^{-1}. Thus, the FT-IR spectrum of the surface film formed in the presence of the inhibitor formulation infers the presence of [Fe(ll)-Inhibitor] complex and small amounts of oxides and hydroxides of Fe (III). The disappearance and the shift of certain peaks to higher wave numbers proved that some interactions have been taking place over the metal surface (Eddy *et al.*, 2010).

Conclusion

The studied compound was realized to be an effective inhibitor for mild steel corrosion in a 2 M HCl solution. The adsorption of this inhibitor on a mild steel surface in 2 M HCl solution follows Temkin adsorption isotherm and is a spontaneous exothermic process accompanied by an increase in entropy. The phenomenon of physical adsorption was proposed from the values of kinetic/thermodynamics parameters obtained. Quantum chemical parameters and local selectivity indices predicted the direction of the inhibition reactions and the sites for nucleophilic/electrophilic attacks concerning the studied inhibitors. Quantum chemical calculations also reveal that apart from studied compound molecules adsorbing as cationic species on the mild steel surface, they can also adsorb as molecular species using oxygen, nitrogen, and benzylic carbons as their active centers. FT-IR spectroscopy was utilized to understand the process of rusting of mild steel. The FT-IR spectrum of the surface film formed in the presence of the inhibitor formulation infers the presence of [Fe(ll)-Inhibitor] complex and small amounts of oxides and hydroxides of Fe(lll).

Compliance with ethical standards

Acknowledgments: The authors wish to express deep appreciation to the Akwa Ibom State University, Mkpat Enin, Nigeria for providing facilities for this study.

Disclosure of conflict of interest: The authors declare no conflicts of interest.

References

Abd El Rehim, S.S., Ibrahim, M.A.M., Khalid, K.F., 2001. The inhibition of 4-(2′-amino-5′-methylphenylazo) antipyrine on corrosion of mild steel in HCl solution. *Mater. Chem. Phys.* 70, 268–273. https://doi.org/10.1016/S0254-0584(00)00462-4

Antonijević, M.M., Milić, S.M., Petrović, M.B., 2009. Films formed on copper surfaces in chloride media in the presence of azoles. *Corros. Sci.* 51, 1228–1237.

Anusuya, N., Sounthari, P., Saranya, J., Parameswari, K., Chitra, S., 2015. Quantum chemical study on the corrosion inhibition property of some heterocyclic azole derivatives. *Orient. J. Chem.* 31, 1741.

Batah A., Anejjar A., Belkhaouda M., Bammou L., Salghi R., Bazzi L., Hammouti B., Chetouani A. (2017), Electrochemical and thermodynamic study of the inhibitory efficacy of Methanol extracts of the Rind and Leaves of Grapefruit plant on the corrosion of carbon steel in an acidic medium, *Mor. J. Chem.* 5 N°3, 404-416

Benzai A., Derridj F., El Ati R., El Kodadi M., Touzani R., Aouniti A., Hammouti B., Ben Hadda T., Doucet H. (2019) Studies of Catecholase Activities of N-donor Bidentates Ligands derivated from Benzoxazole with Copper (II) Salts, *Mor. J. Chem.* 7 N°2, 401-409

Benzai A., Derridj F., Mouadili O., El Azzouzi M., Kaddouri M., Cherrak K., Touzani R., Aouniti A., Hammouti B., Elatki R. (2021). Anti-corrosive properties and quantum chemical studies of (benzoxazol) derivatives on mild steel in HCl (1 M). *Port. Electrochim. Acta* 39, 129–147.

Bouklah M., Ouassini K., Hammouti B., El Idrissi A. (2006), Corrosion inhibition of steel in sulphuric acid by pyrrolidine derivatives, *Appl. Surf. Sci.,* 252 N°6, 2178-2185.

Boulhaoua, M., El Hafi, M., Zehra, S., Eddaif, L., Alrashdi, A.A., Lahmidi, S., Guo, L., Mague, J.T., Lgaz, H., 2021. Synthesis, structural analysis and corrosion inhibition application of a new indazole derivative on mild steel surface in acidic media complemented with DFT and MD studies. *Colloids Surfaces A Physicochem. Eng. Asp.* 617, 126373.

Chauhan, D.S., Quraishi, M.A., Qurashi, A., 2021. Recent trends in environmentally sustainable Sweet corrosion inhibitors. *J. Mol. Liq.* 326, 115117.

Cherrak, K., El Massaoudi, M., Outada, H., Taleb, M., Lgaz, H., Zarrouk, A., Radi, S., Dafali, A., 2021. Electrochemical and theoretical performance of new synthetized pyrazole derivatives as promising corrosion inhibitors for mild steel in acid environment: Molecular structure effect on efficiency. *J. Mol. Liq.* 342, 117507.

Deng, S., Li, X., Xie, X., 2014. Hydroxymethyl urea and 1, 3-bis (hydroxymethyl) urea as corrosion inhibitors for steel in HCl solution. *Corros. Sci.* 80, 276–289. https://doi.org/10.1016/j.corsci.2013.11.041

Dohare, P., Quraishi, M.A., Verma, C., Lgaz, H., Salghi, R., Ebenso, E.E., 2019. Ultrasound induced green synthesis of pyrazolo-pyridines as novel corrosion inhibitors useful for industrial pickling process: Experimental and theoretical approach. *Results Phys.* 13, 102344.

Ebenso, E.E., Isabirye, D.A., Eddy, N.O., 2010. Adsorption and quantum chemical studies on the inhibition potentials of some thiosemicarbazides for the corrosion of mild steel in acidic medium. *Int. J. Mol. Sci.* 11, 2473–2498. https://doi.org/10.3390/ijms11062473

Echihi, S., Benzbiria, N., Belghiti, M.E., El Fal, M., Boudalia, M., Essassi, E.M., Guenbour, A., Bellaouchou, A., Tabyaoui, M., Azzi, M., 2021. Corrosion inhibition of copper by pyrazole pyrimidine derivative in synthetic seawater: experimental and theoretical studies. *Mater. Today Proc.* 37, 3958–3966.

Eddy, N.O., 2011. Experimental and theoretical studies on some amino acids and their potential activity as inhibitors for the corrosion of mild steel, part 2. *J. Adv. Res.* 2, 35–47. https://doi.org/10.1016/j.jare.2010.08.005

Eddy, N.O., 2010. Part 3. Theoretical study on some amino acids and their potential activity as corrosion inhibitors for mild steel in HCl. *Mol. Simul.* 36, 354–363. https://doi.org/10.1080/08927020903483270

Eddy, N.O., Ebenso, E.E., Ibok, U.J., 2010. Adsorption, synergistic inhibitive effect and quantum chemical studies of ampicillin (AMP) and halides for the corrosion of mild steel in H2SO4. *J. Appl. Electrochem.* 40, 445–456. https://doi.org/10.1007/s10800-009-0015-z

Eddy, N.O., Momoh-Yahaya, H., Oguzie, E.E., 2015. Theoretical and experimental studies on the corrosion inhibition potentials of some purines for aluminum in 0.1 M HCl. *J. Adv. Res.* 6, 203–217. https://doi.org/10.1016/j.jare.2014.01.004

El-Hajjaji, F., Belghiti, M.E., Hammouti, B., Jodeh, S., Hamed, O., Lgaz, H., Salghi, R., 2018. Adsorption and corrosion inhibition effect of 2-mercaptobenzimidazole (surfactant) on a carbon steel surface in an acidic medium: Experimental and monte carlo simulations. *Port. Electrochim. Acta* 36, 197–212.

El Arrouji, S., Alaoui, K.I., Zerrouki, A., Kadiri, S.E.L., Touzani, R., Rais, Z., Baba, M.F., Taleb, M., Chetouani, A., Aouniti, A., 2016. The influence of some pyrazole derivatives on the corrosion behaviour of mild steel in 1M HCl solution. *J. Mater. Environ. Sci* 7, 299–309.

El Arrouji, S., Karrouchi, K., Berisha, A., Alaoui, K.I., Warad, I., Rais, Z., Radi, S., Taleb, M., Zarrouk,

A., 2020. New pyrazole derivatives as effective corrosion inhibitors on steel-electrolyte interface in 1 M HCl: Electrochemical, surface morphological (SEM) and computational analysis. *Colloids Surfaces A Physicochem. Eng. Asp.* 604, 125325.
El Ouadi, Y., Lamsayah, M., Bendaif, H., Benhiba, F., Touzani, R., Warad, I., Zarrouk, A., 2021. Electrochemical and theoretical considerations for interfacial adsorption of novel long chain acid pyrazole for mild steel conservation in 1 M HCl medium. *Chem. Data Collect.* 31, 100638.
Emranuzzaman, Kumar, T., Vishwanatham, S., Udayabhanu, G., 2004. Synergistic effects of formaldehyde and alcoholic extract of plant leaves for protection of N80 steel in 15% HCl. *Corros. Eng. Sci. Technol.* 39, 327–332. https://doi.org/10.1179/174327804X13181
Essien, K.E., Abai, E.J., 2022. Corrosion Inhibition Potential of Two Isoxazole Derivatives: Experimental and Theoretical Analyses. *J. Mater. Environ. Sci.,* 13, Issue 08, 928-944
Fouda, A.S., Abd El-Aal, A., Kandil, A.B., 2006. The effect of some phthalimide derivatives on corrosion behavior of copper in nitric acid. *Desalination* 201, 216–223. https://doi.org/10.1016/j.desal.2005.11.030
Fouda, A.S., Ellithy, A.S., 2009. Inhibition effect of 4-phenylthiazole derivatives on corrosion of 304L stainless steel in HCl solution. *Corros. Sci.* 51, 868–875.
Glaser, R., Lewis, M., Wu, Z., 2000. Stereochemistry and stereoelectronics of azines. 13. Conformational effects on the quadrupolarity of azines. An ab initio quantum-mechanical study of a lateral synthon. *Mol. Model. Annu.* 6, 86–98.
Guendouz, A., Missoum, N., Chetouani, A., Al-Deyab, S.S., Cheikhe, B. Ben, Boussalah, N., Aouniti, A., 2013. Quantum chemical studies on the inhibiting effect of new synthesized bipyrazols of C38 steel corrosion in 1M HCl. *Int J Electrochem Sci* 8, 4305–4327.
Hosseini, S.M.A., Salari, M., Jamalizadeh, E., Khezripoor, S., Seifi, M., 2010. Inhibition of mild steel corrosion in sulfuric acid by some newly synthesized organic compounds. *Mater. Chem. Phys.* 119, 100–105. https://doi.org/10.1016/j.matchemphys.2009.08.029
Ikot, A.N., Akpabio, L.E., Essien, K., Ituen, E.E., Obot, I.B., 2009. Variational principle techniques and the propertiesof a cut-off and anharmonic wave function. E-Journal Chem. 6, 113–119.
Ishii, M., Nakahira, M., Yamanaka, T., 1972. Infrared absorption spectra and cation distributions in (Mn, Fe) 3O4. *Solid State Commun.* 11, 209–212.
Jackson, E., Essien, K.E., 2019. Experimental and Theoretical Approach of L-Methionine Sulfone (LMS) as corrosion inhibitor for mild steel in HCL Solution. *Environment* 1, 2.
Jackson, E., Essien, K.E., Okafor, P.C., 2016. Experimental and Quantum Studies: A New Corrosion Inhibitor for Mild Steel. *Elixir Corrosion and Dye* 86, 34978–34983
Ji, Y., Xu, B., Gong, W., Zhang, X., Jin, X., Ning, W., Meng, Y., Yang, W., Chen, Y., 2016. Corrosion inhibition of a new Schiff base derivative with two pyridine rings on Q235 mild steel in 1.0 M HCl. *J. Taiwan Inst. Chem. Eng.* 66, 301–312.
Khaled, K.F., Abdel-Rehim, S.S., Sakr, G.B., 2012. On the corrosion inhibition of iron in hydrochloric acid solutions, Part I: Electrochemical DC and AC studies. *Arab. J. Chem.* 5, 213–218. https://doi.org/10.1016/j.arabjc.2010.08.015
Li, X., Deng, S., Xie, X., Fu, H., 2014. Inhibition effect of bamboo leaves' extract on steel and zinc in citric acid solution. *Corros. Sci.* 87, 15–26. https://doi.org/10.1016/j.corsci.2014.05.013
Mechbal, N., Belghiti, M.E., Benzbiria, N., Lai, C.-H., Kaddouri, Y., Karzazi, Y., Touzani, R., Zertoubi, M., 2021. Correlation between corrosion inhibition efficiency in sulfuric acid medium and the molecular structures of two newly eco-friendly pyrazole derivatives on iron oxide surface. *J. Mol. Liq.* 331, 115656.
Misawa, T., Asami, K., Hashimoto, K., Shimodaira, S., 1974. The mechanism of atmospheric rusting and the protective amorphous rust on low alloy steel. *Corros. Sci.* 14, 279–289.
Misawa, T., Kyuno, T., Suetaka, W., Shimodaira, S., 1971. The mechanism of atmospheric rusting and the effect of Cu and P on the rust formation of low alloy steels. *Corros. Sci.* 11, 35–48.
Njoku, D.I., Onuoha, G.N., Oguzie, E.E., Oguzie, K.L., Egbedina, A.A., Alshawabkeh, A.N., 2019. Nicotiana tabacum leaf extract protects aluminium alloy AA3003 from acid attack. *Arab. J. Chem.*

12, 4466–4478. https://doi.org/10.1016/j.arabjc.2016.07.017
Njoku, D.I., Ukaga, I., Ikenna, O.B., Oguzie, E.E., Oguzie, K.L., Ibisi, N., 2016. Natural products for materials protection: corrosion protection of aluminium in hydrochloric acid by Kola nitida extract. *J. Mol. Liq.* 219, 417–424. https://doi.org/10.1016/j.molliq.2016.03.049
Obi-Egbedi, N.O., Essien, K.E., Obot, I.B., 2011a. Computational simulation and corrosion inhibitive potential of alloxazine for mild steel in 1M HCl. *J. Comput. Methods Mol. Des.* 1, 26–43.
Obi-Egbedi, N.O., Essien, K.E., Obot, I.B., Ebenso, E.E., 2011b. 1, 2-Diaminoanthraquinone as corrosion inhibitor for mild steel in hydrochloric acid: weight loss and quantum chemical study. *Int. J. Electrochem. Sci* 6, 913–930.
Obot A.S., Boekom E.J., Ituen E.B., Ugi B.U., Essien K.E., Jonah N.B. (2021). Thermodynamic investigation and quantum chemical evaluation of n-hexane extracts of Costus lucanusianus as corrosion inhibitors for mild steel and aluminum in 1 M HCl solution. *J. Appl. Phys. Sci. Int.* 13, 6–27.
Obot, I.B., Obi-Egbedi, N.O., 2010. Theoretical study of benzimidazole and its derivatives and their potential activity as corrosion inhibitors. Corros. Sci. 52, 657–660.
Obot, I.B., Obi-Egbedi, N.O., 2008. Fluconazole as an inhibitor for aluminium corrosion in 0.1 M HCl. Colloids surfaces a Physicochem. Eng. Asp. 330, 207–212. https://doi.org/10.1016/j.colsurfa.2008.07.058
Obot, I.B., Obi-Egbedi, N.O., Odozi, N.W., 2010. Acenaphtho [1, 2-b] quinoxaline as a novel corrosion inhibitor for mild steel in 0.5 M H2SO4. *Corros. Sci.* 52, 923–926. https://doi.org/10.1016/j.corsci.2009.11.013
Oguzie, E.E., Adindu, C.B., Enenebeaku, C.K., Ogukwe, C.E., Chidiebere, M.A., Oguzie, K.L., 2012. Natural products for materials protection: mechanism of corrosion inhibition of mild steel by acid extracts of Piper guineense. *J. Phys. Chem. C* 116, 13603–13615. https://doi.org/10.1021/jp300791s
Ouchrif, A., Zegmout, M., Hammouti, B., El-Kadiri, S., Ramdani, A., 2005. 1, 3-Bis (3-hyroxymethyl-5-methyl-1-pyrazole) propane as corrosion inhibitor for steel in 0.5 M H2SO4 solution. *Appl. Surf. Sci.* 252, 339–344.
Paul, P.K., Yadav, M., Obot, I.B., 2020. Investigation on corrosion protection behavior and adsorption of carbohydrazide-pyrazole compounds on mild steel in 15% HCl solution: Electrochemical and computational approach. *J. Mol. Liq.* 314, 113513.
Rahmani, H., El-Hajjaji, F., El Hallaoui, A., Taleb, M., Rais, Z., El Azzouzi, M., Labriti, B., Ismaily, A.K., Hammouti, B., 2018. Experimental, quantum chemical studies of oxazole derivatives as corrosion inhibitors on mild steel in molar hydrochloric acid medium. *Int. J. Corros. Scale Inhib.* 7, 509–527.
Rguiti M. M., Chadili M., El Ibrahimi B., Baddouh A., Bazzi Lh., Hilali M. and Bazzi L. (2018) Iron corrosion inhibition by olive mill wastewaters in acid medium, *Mor. J. Chem*. 6 N°2 (2018) 307-317
Solomon, M.M., Essien, K.E., Loto, R.T., Ademosun, O.T., 2022. Synergistic corrosion inhibition of low carbon steel in HCl and H2SO4 media by 5-methyl-3-phenylisoxazole-4-carboxylic acid and iodide ions. J. Adhes. Sci. Technol. 36, 1200–1226.
Soltani, N., Tavakkoli, N., Kashani, M.K., Mosavizadeh, A., Oguzie, E.E., Jalali, M.R., 2014. Silybum marianum extract as a natural source inhibitor for 304 stainless steel corrosion in 1.0 M HCl. *J. Ind. Eng. Chem.* 20, 3217–3227. https://doi.org/10.1016/j.jiec.2013.12.002
Tang, L., Li, X., Mu, G., Liu, G., Li, L., Liu, H., Si, Y., 2006. The synergistic inhibition between hexadecyl trimethyl ammonium bromide (HTAB) and NaBr for the corrosion of cold rolled steel in 0.5 M sulfuric acid. *J. Mater. Sci.* 41, 3063–3069. https://doi.org/10.1007/s10853-006-6987-8
Tebbji, K., Oudda, H., Hammouti, B., Benkaddour, M., El Kodadi, M., Ramdani, A., 2005. Inhibition effect of two organic compounds pyridine–pyrazole type in acidic corrosion of steel. *Colloids Surfaces A Physicochem. Eng.* Asp. 259, 143–149.
Tebbji K., Bouabdellah I., Aouniti A., Hammouti B., Oudda H., Benkaddour M., Ramdani A. (2007),

N-benzyl-N,N-bis[(3,5-dimethyl-1H-pyrazol-1-yl)methyl]amine as corrosion inhibitor of steel in 1 M HCl, *Mater. Let.* 61N°3, 799-804.
Udhayakala, P., Rajendiran, T. V, Gunasekaran, S., 2012. Theoretical approach to the corrosion inhibition efficiency of some pyrimidine derivatives using DFT method. *J. Comput. Methods Mol. Des.* 2, 1–15.
Umoren, S.A., 2011. Synergistic inhibition effect of polyethylene glycol–polyvinyl pyrrolidone blends for mild steel corrosion in sulphuric acid medium. *J. Appl. Polym. Sci.* 119, 2072–2084. https://doi.org/10.1002/app.32922
Umoren, S.A., 2008. Inhibition of aluminium and mild steel corrosion in acidic medium using Gum Arabic. *Cellulose 1*5, 751–761. https://doi.org/10.1007/s10570-008-9226-4
Verma, C., Saji, V.S., Quraishi, M.A., Ebenso, E.E., 2020. Pyrazole derivatives as environmental benign acid corrosion inhibitors for mild steel: experimental and computational studies. *J. Mol. Liq.* 298, 111943.
Yadav, M., Behera, D., Kumar, S., 2014. Experimental and theoretical studies on corrosion inhibition of mild steel in hydrochloric acid by thiosemicarbazone of Schiff bases. *Can. Metall. Q.* 53, 220–231. https://doi.org/10.1179/1879139513Y.0000000118
Yadav, M., Gope, L., Kumari, N., Yadav, P., 2016. Corrosion inhibition performance of pyranopyrazole derivatives for mild steel in HCl solution: Gravimetric, electrochemical and DFT studies. *J. Mol. Liq.* 216, 78–86.